Supplementary Materials:

Meta-Analysis Comparing Wettability Parameters and the Effect of Wettability on Friction Coefficient in Lubrication

Michael J. Schertzer * and Patricia Iglesias

Department of Mechanical Engineering, Rochester Institute of Technology, Rochester, NY 14623, USA; pxieme@rit.edu
* Correspondence: mjseme@rit.edu; Tel.: +1-585-475-5715

Characterization of friction factor using $\lambda \cdot |S^{**}|$ (Figure S1) gives similar results to the characterization with $\lambda \cdot |S^{*}|$ (Figure 6). Separations of cases for apparent film ($\lambda \cdot |S^{**}| > 1$), boundary ($\lambda \cdot |S^{**}| < 10^{-3}$), and transitional ($10^{-3} < \lambda \cdot |S^{**}| < 1$) lubrication occurred for similar ranges of $\lambda \cdot |S^{**}|$. While the characterizations are similar, it is worth noting that $|S^{**}|$ requires more input parameters than $|S^{*}|$.

Multiplying λ by the dimensionless spreading parameter SP^{**} does not provide the same insight as $\lambda \cdot |S^{*}|$ (Figure 6) or $\lambda \cdot |S^{**}|$ Figure S1. When adhesion is greater than cohesion, S^{*} and S^{**} become small negative numbers, but SP^{*} and SP^{**} change sign. Since the sign of SP^{*} and SP^{**} changes, taking the absolute value of either parameter reduces the information they provide.

The ratio of cohesion work to adhesion work (W_C/W_A) is another potential dimensionless parameter to describe wetting between a lubricant and a target surface. This ratio can be formulated as a function of the contact angle

$$\frac{W_{C,\theta}}{W_{A,\theta}} \approx \frac{2}{\cos\theta + 1}, \tag{S1a}$$

or a function of the disperse and polar coordinates of the surface tension and surface energy

$$\frac{W_{C,DP}}{W_{A,DP}} \approx \frac{1}{\sqrt{\frac{\gamma_S^D \gamma_L^D}{\gamma_{lm}^2}} + \sqrt{\frac{\gamma_S^P \gamma_L^P}{\gamma_{lm}^2}}}. \tag{S2b}$$

Like the dimensionless spreading parameters, $W_{C,\theta}/W_{A,\theta}$ and $W_{C,DP}/W_{A,DP}$ were correlated to contact angle (Figure S2a) and linearly correlated with each other (Figure S2b). Like S, S^{*}, and S^{**}, the sign of this ratio does not change with θ and the absolute value increases with increasing contact angle. Like S^{*}, $W_{C,\theta}/W_{A,\theta}$ can be fully determined with a measurement of the contact angle between the lubricant and the target surface.

The ratio of cohesive to adhesive energy (W_C/W_A) can can also be used to try to capture the effect of wettability on friction coefficient (Figure S3). Similar regimes are seen on this figure with hydrodynamic lubrication occurring when $\lambda \cdot (W_C/W_A) > 1$, and moderate and dramatic changes to friction coefficient in the regions defined by ($0.01 < \lambda \cdot (W_C/W_A) < 1$), and when $\lambda \cdot (W_C/W_A) < 1$, respectively. On this figure, the cases where IL 104 was used as a lubricant for Steel-Steel and POM-POM contact fall in at the beginning the transitional region instead of the end of the boundary lubrication region. Like $|S^{*}|$, it is possible to calculate (W_C/W_A) with only θ (Figure S2b).

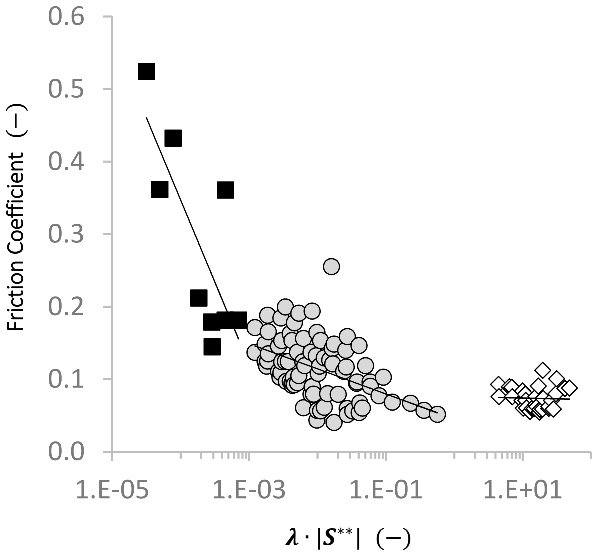

Figure S1. Friction coefficient as a function of lambda multiplied by the dimensionless spreading parameter $(\lambda \cdot |S^{**}|)$. Data includes cases from [7] where $(\lambda \cdot |S^{**}|) > 1$ (white), $(\lambda \cdot |S^{**}|) < 0.001$ (black), and $0.01 < (\lambda \cdot |S^{**}|) < 1$ (gray).

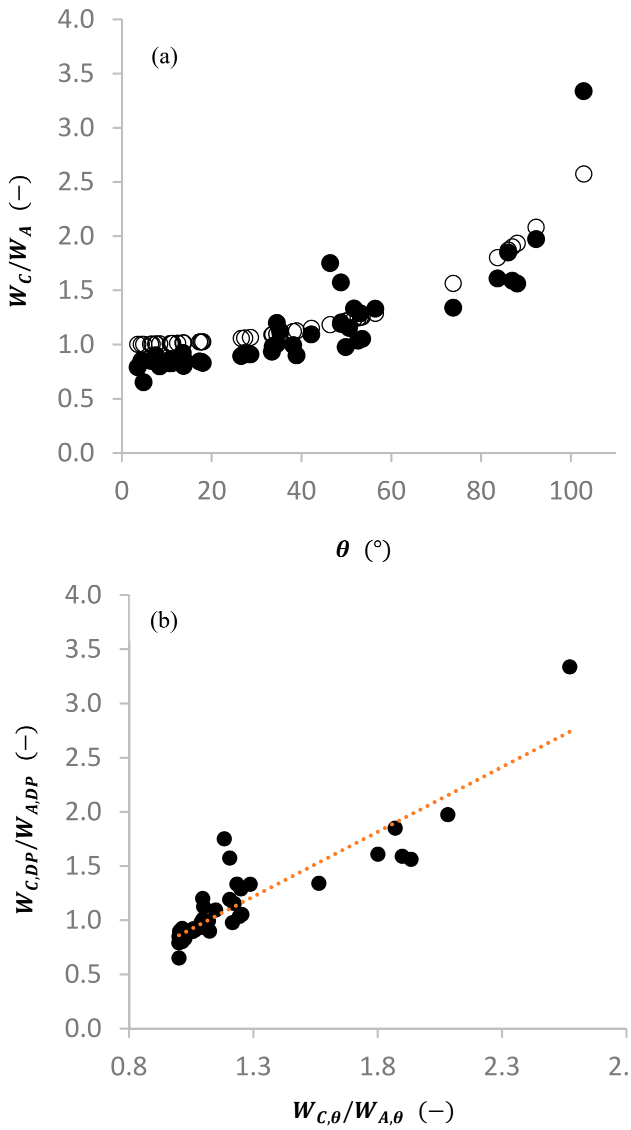

Figure S2. Comparison of (a) $W_{C,DP}/W_{A,DP}$ (closed) and $W_{C,\theta}/W_{A,\theta}$ (open) to the θ and (b) a direct comparison of $W_{C,DP}/W_{A,DP}$ and $W_{C,\theta}/W_{A,\theta}$ for experimental cases in [7,10,16]

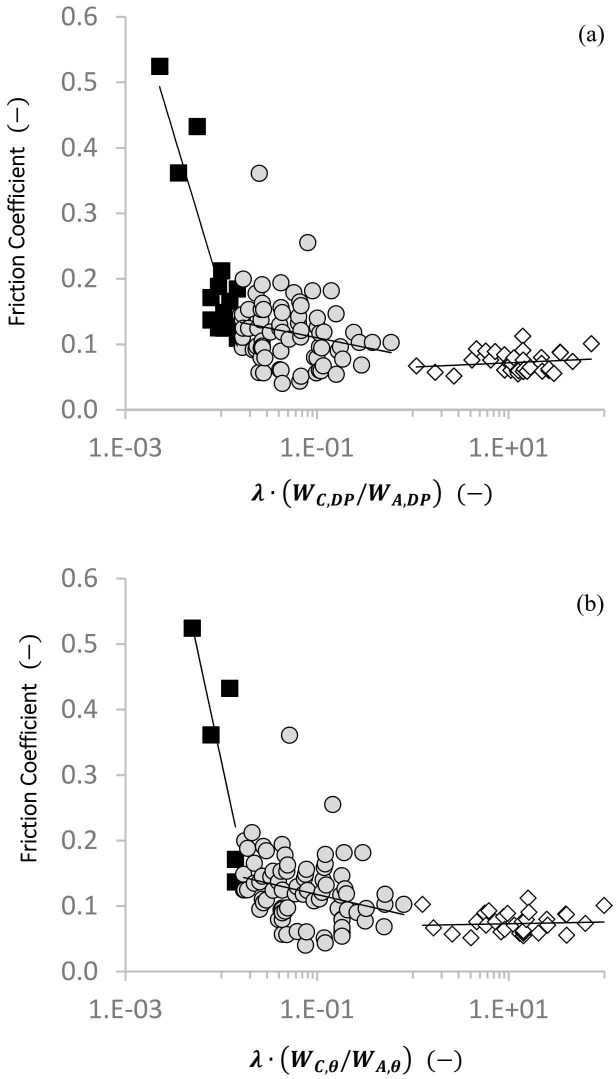

Figure S3. Friction coefficient as a function of lambda multiplied by the ratio of cohesion to adhesion formulated using (a) polar and disperse components of surface tension and (b) contact angles. Data includes cases from [7] where $(W_C/W_A) > 1$ (white), $(W_C/W_A) < 0.015$ (black), and $0.0125 < (W_C/W_A) < 1$ (gray). Log fits in each regime are provided.